

## Noble Metal Nanoparticles and Their (Bio) Conjugates. II. Preparation

Ignác Capek

Correspondence: Ignác Capek, Slovak Academy of Sciences, Polymer Institute, Institute of Measurement Science, Dúbravská cesta, Bratislava and Faculty of Industrial Technologies, TnUni, Púchov, Slovakia

Received: February 3, 2015 Accepted: August 24, 2015 Online Published: January 6, 2016

doi:10.5539/ijc.v8n1p86

URL: <http://dx.doi.org/10.5539/ijc.v8n1p86>

### Abstract

Hybrid nanoparticles of gold and silver can not only retain the beneficial features of both nanomaterials, but also possess unique advantages (synergism) over the other two types. Novel pseudospherical and anisotropic nanoparticles, bimetallic triangular nanoparticles, and core@shell nanoparticles were prepared by the different procedures for various applications and understanding both the particle evolution (nucleation) and nanoparticle anisotropy. Hybrid nanoparticles of gold and silver are considered to be low in toxicity, and exhibit facile surface functionalization chemistry. Furthermore, their absorption peaks are located in visible and near-infrared region. These nanoparticles provide significant plasmon tunability, chemical and surface modification properties, and significant advances in the growth into anisotropic nanostructures. The photoinduced synthesis can be used to prepare various (sub) nanoparticles and OD and 1D nanoparticles. Ostwald and digestive ripening provided narrower particle size distribution.

**Keywords:** functional, hybrid, core@shell, bimetallic and (an) isotropic noble metal nanoparticles, Oswaldt and digestive ripening process

### 1. Introduction

The noble metal nanoparticle colloids were reported to exhibit a wide range of various applications from different fluids to in vitro and vivo as a carrier for drug delivery into cells and tissues to optical and magnetic manipulations in biomedical systems as well (Sun et al., 2000). The unique physical and chemical properties of nanoparticles are given by their large surface area or a large surface-to-volume ratio and high reactivity. The unique optical and magnetic properties of nanoparticles are controlled by the type of atoms (metals), composition of nanoparticles, particle shape, type and concentration of functional groups and so on (Feldmann, 2003). For example, the composite nanoparticles with the iron atoms domains generate the magnetism and with the gold atoms exhibit the unique optical features. Therefore such nanoparticles exhibit unique properties which mostly strongly differ from the bulk or classical materials.

The future generation of environmental nanotechnologies based on noble metal nanoparticles is supposed to replace conventional environmental technologies by novel nano(bio)technologies (Modi, et al., 2003). Zero- and one-dimensional (OD and 1D) nanoparticles and two- and three (2D and 3D) nanoparticle assays belong to these unique nanomaterials. Especially the nanostructures decorated with different (bio) molecules are exceptional materials with nonconventional such as biomedical harvesting properties.

Polymer- or biopolymer decorated metal nanoparticles are prepared by several procedures with and without templates. Most existing procedures explore the strong affinity of alkylthiol ligands and surfactants to gold and silver (Brust et al., 1994), the use of alkyl or aryl derivatives of disulfides (Shon et al., 2001), and thioethers (Li et al., 2001) as well. Furthermore, organic compounds with polar groups (Boal et al., 2000), thioacetate groups (Brousseau et al., 1999), amino- and carboxylate groups and tetradentate thioether ligands (Maye et al., 2002) have recently been used to mediate the formation of OD or 1D nanoparticles. In this second part of the review (Preparation II) we summarize and discuss the preparation hybrid, functional and bimetallic noble metal nanoparticles including their particle nucleation, ripening and optical properties.

### 2. Hybrid Nanoparticles

Hybrid nanoparticles are composed of different inorganic and organic components that can not only retain the beneficial features of both nanomaterials, but also possess unique advantages (synergism) over the other two types. For example, the ability to combine a multitude of organic and inorganic components in a modular fashion allows for systematic tuning of the properties of the resultant hybrid nanomaterial. Currently, there are four common synthetic strategies to prepare hybrid nanoparticles. The first strategy involves the preparation of each component particle separately and then

both (or all) components were incorporated into micrometer size porous bead (Sathe et al., 2006), polymeric micelle (Park et al., 2008), silica core or shell matrix (Gole et al., 2008) or alternate polymeric layers (Kulakovich et al., 2002). In the second approach one of the presynthesized particles is coated with polymer of desired thickness and then attached with other presynthesized nanoparticles (Zhai et al., 2009). In the third approach the seed nanoparticle is prepared first, and then it is used to grow with other atoms (Selvan et al., 2007; Jiang et al., 2008). In the last approach each presynthesized component particle is functionalized first, and then hybrid particles are prepared by chemical/biochemical linkage (Pons et al., 2007; Fu et al., 2009). In the first two methods the large composite nanoparticles (>50 nm to micrometer size) with a resultant poor colloidal stability are formed. The third approach, on the contrary, provides small nanoparticles (Selvan et al., 2007). The last procedure provides small nanoparticles with the low yield and often mixed with nanoparticle side products and requires some separation methods (Fu et al., 2004).

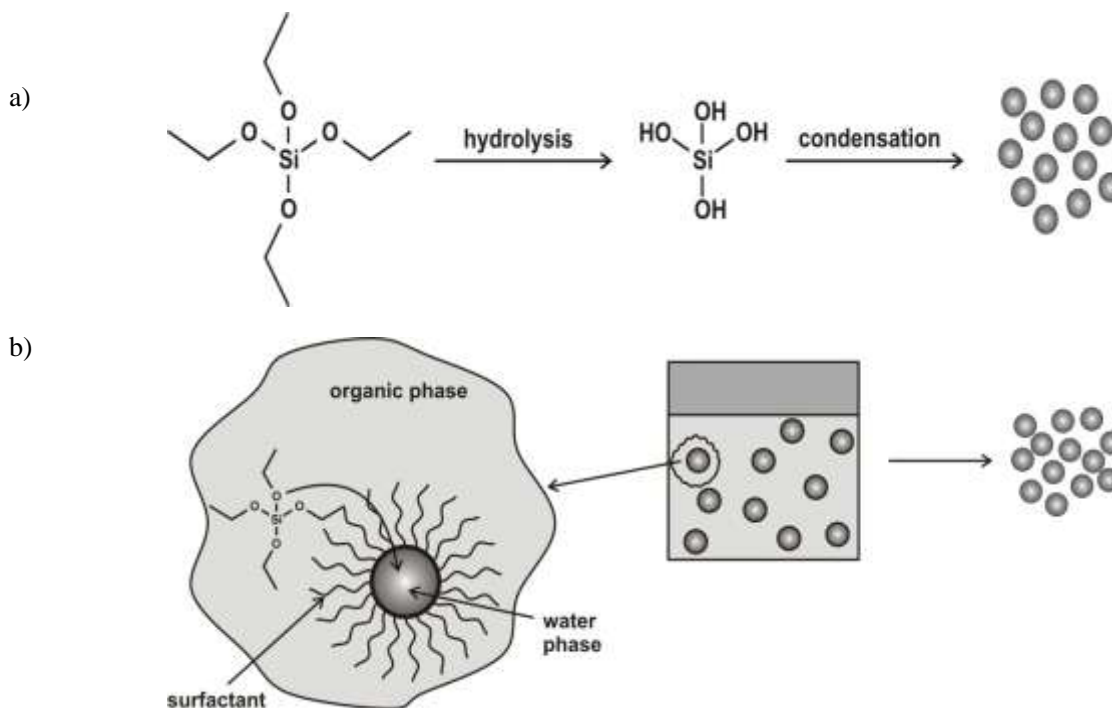
Hybrid nanoparticles of gold and silver are considered to be low in toxicity, and exhibit facile surface functionalization chemistry (Jain et al., 2008). Furthermore, their absorption peaks are located in visible and near-infrared region. Hybrid gold/silver nanoparticles provide significant plasmon tunability, chemical and surface modification properties, and significant advances in the growth into anisotropic nanostructures (Xiang et al., 2008). Novel pseudospherical and anisotropic nanoparticles, bimetallic triangular nanoparticles, and core@shell nanoparticles were prepared by the different (above mentioned) procedures for various applications and understanding both the particle evolution (nucleation) and nanoparticle anisotropy (Xue et al., 2007). The photoinduced synthesis of noble metal nanoparticles is broadly used approach to initiate photochemical reduction processes leading to oligomers, subnanoparticles and OD and 1D nanoparticles. Xue et al. have used the photochemical approach for the preparation of Au@Ag OD and 1D (nanorods, nanoprisms) nanoparticles and explained the mechanism of the photochemical growth of silver nanoprisms using spherical metal seeds (Xue et al., 2007).

Anisotropic hybrid nanoparticles can be also prepared by several approaches. One of them is a microemulsion. Herein the mixing of single microemulsions can tune the final structure and composition of final nanoparticles (Capek, 2004; Glomm, 2005; Hunter, 2004; Murphy & Jana, 2002). The second approach is based on the (co)deposition of atoms or primary metal nanoparticles onto seeds and their encapsulation within the various templates. Co-deposition of small gold nanoparticles onto nanowires or encapsulation of gold nanoparticles or their atoms within metal colloids was used to prepare desired anisotropic nanostructures (Hu et al., 2006). This approach can be used to vary the colloidal and collective properties of 1D nanomaterials, for example, the transformation of gold spherical nanoparticles onto 1D nanoparticles (Nam et al., 2006). Core@shell nanoparticles belong to the unique composite nanostructures. They can be prepared by various procedures, for example, by the reduction of two or more metal salts with different reactivity in solutions. The reduction of most reactive metal salts leads to the formation of particle core and the postponed reduction of other salt can form the atoms or primary nanoparticles that deposit onto the preformed nanoparticles. The seed nanoparticles can also be used as a solid matrix or template for the deposition of other present atoms. This procedure was used to prepare various ferromagnetic or plasmonic/magnetic nanostructures such as gold@cobalt, gold@Fe<sub>x</sub>O<sub>y</sub>, and so on, nanoparticles with a nondipolar gold core and a ferromagnetic cobalt (iron oxide) shell (Yu et al., 2005; Korth et al., 2008). The gold@cobalt nanoparticles were prepared by the thermolysis of Co<sub>2</sub>(CO)<sub>8</sub> in the presence of the oleylamine-capped gold nanoparticles as seeds. The amine-terminated oligopolystyrene (OPS) surfactants were used for the stabilization of these hybrid nanostructures. TEM and HRTEM confirmed the presence of OPS-capped Au@Co nanostructures by the formation of larger (d ~ 22 nm) nanoparticles compared to the AuNP seeds. These particle nanostructures self-assembled into the mesoscopic nanoparticle chains spanning hundreds of nanometers to micrometers in length. HRTEM further confirmed the formation of hybrid OPS-capped Au@CoNPs by the imaging of a discrete core@shell morphology composed of the darker high-atomic-number gold nanoparticle core (d<sub>core</sub> ~ 13 nm) and a lighter shell from the metallic cobalt (thickness ~ 4-5 nm).

A heterogeneous nucleation of composite noble metal nanoparticle is based on the mixing of a precursor (salt, reductant and additives) solution with a micelle solution saturated with the seed metal nanoparticles (Lin et al., 1999a). This procedure was used to prepare sets of metal composite nanoparticles. Herein the inverse cationic micelles were used to grow the seeds as the feedstock. These hybrid nanoparticles of silver and gold were also prepared by Wilcoxon and Provencio (Wilcoxon & Provencio, 2004). The red colored initial solution with gold nanoparticles with an absorbance peak at 518 nm blue shifts as thicker shells of silver are formed around the core (gold seed) and the core@shell nanostructure appeared. The formation of silver shell is accompanied by yellowing the gold@silver nanoparticles solution with a narrow symmetrical plasmon typical for the silver nanocluster. In the reverse approach (gold deposition onto silver seed nanoparticles - silver@gold nanoparticles), the absorbance peak shifts in the opposite manner. It is noteworthy to mention that even when the composite nanoparticles have much larger fraction of atoms of silver (particle core – seed), the damping of the gold plasmon is much stronger than is observed in a pure gold nanoparticle of the same size.

Silica-based nanomaterials and nanoscale metal–organic frameworks (NMOFs) belong to other interesting hybrid nanomaterials (Taylor-Pashow et al., 2010). The former group can be divided into two nanostructures - silica-based hybrid nanomaterials and solid silica particles and mesoporous silica nanoparticles (MSNPs). Both exhibit unique properties such as high surface areas, tunable pore sizes, and large pore volumes and therefore they are used as the drug delivery nanomaterials, imaging agents or therapeutics. Required cargoes can be either directly incorporated in the silica pores or grafted to the outer surface of the solid silica particles via various functional groups. Thus, the MSNPs must be first functionalized and then coupled with imaging or therapeutic agents. Then these conjugates via loading of cargo into the pores, covalent grafting, and co-condensation of siloxy-derived groups are formed. Silica matrixes can serve as a core or shell template for more complex composite nanostructures with noble metal nanoparticles.

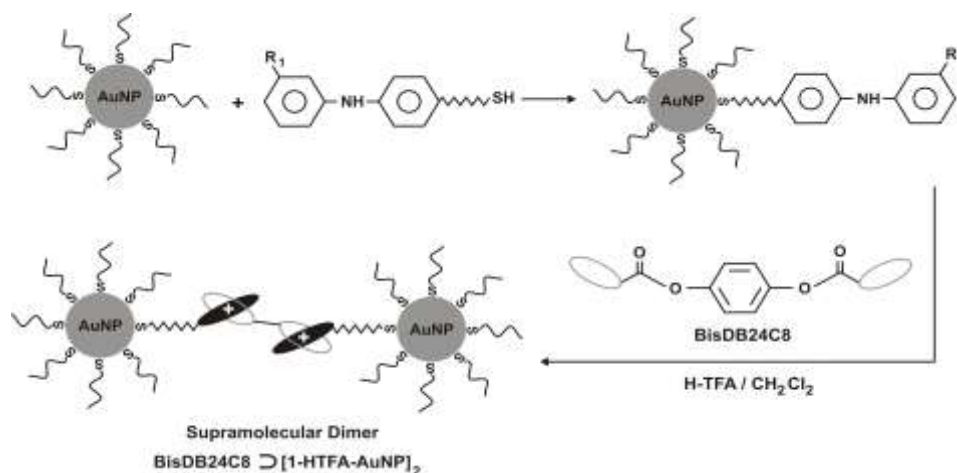
These silica-based nanostructures are mainly synthesized by two approaches: sol–gel and reverse microemulsion. The former approach provides monodisperse solid silica particles ranging in size from 50 nm to 2  $\mu\text{m}$  (Stöber et al., 1968). This synthesis consists of two steps: the hydrolysis and condensation of a silica monomer (tetraethyl orthosilicate (TEOS)) in ethanol solution and as a catalyst is ammonia used (Scheme 5a). The size of the particles can be tuned by variations of precursor concentrations, the type of reaction solvent and temperature. For example, increased the TEOS concentration from 0.05 M to 0.67 M while keeping the other reactant concentrations and conditions constant affords silica particles from 20 to 880 nm in size (Wang et al., 2010). The high stability of silica colloid results from the electrostatic repulsion among the negatively charged silica particles. The second common method for the preparation of silica nanoparticles with narrow particle size distribution is based on the reverse microemulsion that controls simply the kinetics of precursor TEOS hydrolysis, particle nucleation and growth (Scheme 5b) (Rieter et al., 2007). For example, the size and number of final nanoparticles can be tuned by varying the water to surfactant ratio ( $\omega$ ).



Scheme 5. Methods for synthesizing solid silica nanoparticles. (a) The Stöber method, (b) The reverse phase microemulsion (Taylor-Pashow et al., 2010).

Chak et al. have discussed (Chak et al., 2009) the synthesis of composite nanoparticles consisting of small gold nanoparticles (2 nm), dibenzo(24)crown-8 (DB24C8) and dibenzylammonium (DBA). DB24C8 and DBA fragments were connected with the gold nanoparticle via the amine group links, acted as supramolecular recognition motifs and formed form a 1:1 supramolecular complex, namely, (DBA $\subset$ DB24C8) pseudorotaxane (Badjic et al., 2006). The conjugate of amine monofunctional gold nanoparticles (1-AuNPs, decorated with dibenzyl ammonium (DBA)-disulfide ligand) together with a crown-ether-decorated polystyrene resin (PS-DB24C8) and crownether-decorated superparamagnetic iron oxide nanoparticles (SPIO-DB24C8) formed interesting recognition nanomotifs. This research was devoted to the control of the number of active entities per nanoparticle (Grainger & Castner, 2008). Herein, the 1-AuNPs–based smart nanomotifs were formed by self-assembling of supramolecular dimers and trimers bisDB24C8 and trisDB24C8 (Scheme 6). Both the gold-based suprastructures and monofunctional 1-AuNP exhibit the same

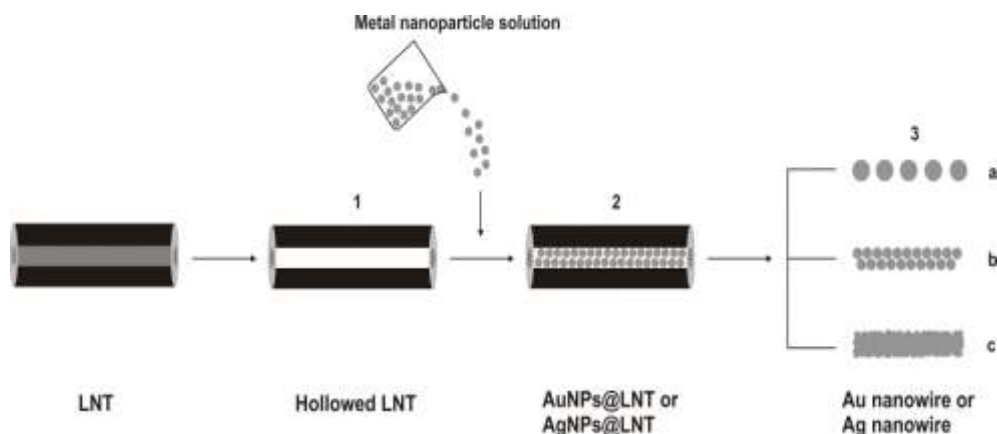
plasmonic band at  $\lambda \sim 520$  nm (Mock et al., 2008). These smart nanoparticle-biomolecule suprastructures with the controlled number of bioentities per nanoparticle, would allow more accurate detection of molecules associated with particular diseases, offering drastic improvements in disease detection, therapy, and prevention (Jain et al., 2008).



Scheme 6. Supramolecular self-assembly of the 1-AuNPs with bisDB24C8 and trisDB24C8 to afford the dimers bisDB24C8 $\supset$ (1 HTFA-AuNP) $_2$  and trimers trisDB24C8 $\supset$ (1 HTFA-AuNP) $_3$ , respectively (Chak et al., 2009).

The further smart suprastructures (hydrogen-bonded supramolecular pseudorotaxane structures) were formed by the conjugation of SPIO-DB24C8 spheres with the functionalized AuNPs. The shell of the suprastructure was formed by gold nanoparticles and its nature was a function of gold particle size. Smaller AuNPs are observed to be well deposited on the periphery of the SPIO-DB24C8 microspheres. The SPIO-DB24C8 microspheres are composed of SPIO nanocrystals confined in thin silica shells, which are decorated with the crown ethers by amide linkages (Chak et al., 2009).

Yang et al. (Yang et al., 2004) have described the fabrication of advanced 1-D metallic organic nanocomposites by loading a vacant lipid nanotubes (LNTs) hollow cylinder with water-soluble gold (AuNPs) and silver nanoparticles (AgNPs) using capillary force (Scheme 7). They achieved the fabrication of gold or silver nanoparticles encapsulated in the cylindrical hollow of the glycolipid nanotube with high-axial ratio by loading the vacant LNT hollow cylinder with aqueous gold or silver nanoparticles using. Aqueous gold or silver nanoparticles (1-3 nm wide) are favorable to form the AuNPs@LNT or AgNPs@LNT nanocomposite in relatively higher yields. This simple and mild approach led to the fabrication of a 1-D metallic-organic nanocomposite loading well defined metallic colloid particles inside the organic nanotube hollow. In addition, the 1-D nanocomposite functions as a convergent template to fabricate a gold nanowire by removing the LNT shell through a firing process. Thus, the fabrication consists of the following steps: (1) Lyophilization of LNTs to empty the internal hollow volume, (2) filling LNTs with aqueous solution containing metal (Au or Ag) nanoparticles, and (3) removing the LNT shell by firing process.

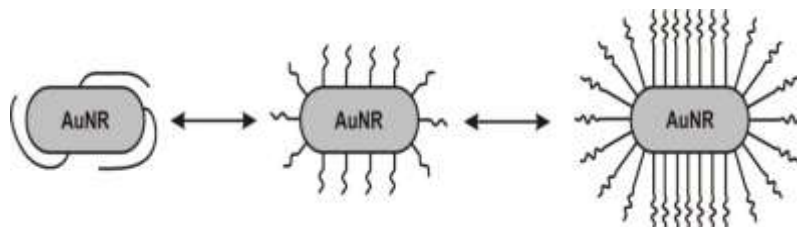


Scheme 7. Schematic diagram for the fabrication of AuNPs@LNT or AgNPs@LNT and a gold nanowire. (1) Lyophilization of LNTs to empty the internal hollow volume, (2) filling LNTs with aqueous solution containing metal (Au or Ag) nanoparticles, and (3) removing the LNT shell by firing process: (a) discrete and (b, c) continuous gold nanowires (Yang et al., 2004).

### 3. Other Nanoparticles

Among valuable noble metal nanoparticles one can find also platinum nanoparticles. The syntheses of platinum nanoparticles of different sizes and shapes such as tetrahedral (Ahmadi, et al., 1996), cubic (Ahmadi, et al., 1996; Fu et al., 2002), nanowire (Chen et al., 2004) and tetrapods (Herricks et al., 2004) have been reported. Platinum nanoparticles were prepared in inverse microemulsions. By mixing of two microemulsions (microdroplets saturated either by precursor such as the platinum salt ( $\text{PtCl}_6^{2-}$ ) or by the reducing agent) started the nucleation and platinum nanoparticles appeared (Ingelsten et al., 2001). The nonionic stabilizers (poly(ethylene glycol)monododecyl ethers ( $\text{C}_{12}\text{E}_4$  (Brij 30),  $\text{C}_{12}\text{E}_5$ ,  $\text{C}_{12}\text{E}_6$ )), anionic stabilizer (sodium bis(2-ethylhexyl)sulfosuccinate (AOT)), and their mixtures were used to formulate the nanoreactors (water-solubilized microdroplets). The reduction of platinum salt is a function of droplet fusion which is given by the type of the palisade stabilizer layer at the droplet surface. The hydrophilic alcohol ethoxylate favors a flux of stabilizer and other reactants back and forth between the bulk hydrocarbon domain and the droplets interface. In contrast, the hydrophobic stabilizer (AOT) favors more elastic collisions and slower rate of fusion of droplets and the formation of smaller nanoparticles (Fletcher et al., 1987). The fusion of droplets is regulated by the composition of interface layer formed by both stabilizers.

Mixtures of hydrophobic AOT and nonionic emulsifiers (based on PEG) were reported to be more efficient than their homo-mixtures in the preparation of platinum nanoparticles (Shelimov et al., 2000). The mechanism of particle formation is also based on the formation mixed micelles or microdroplets and the accumulation of salt precursor in the micelles (microdroplets) via interaction of the polar headgroups of PEG chains and the sulfonate group of AOT with the platinum salt. In the second step the precursor (hexachloroplatinic complex) is reduced by the reducing agent via the droplet scission. The chemisorption of functional surfactants on the particle surface or on the atom aggregates leads to the inhibition of both particle growth and agglomeration and the stable nanoparticles can be fabricated. Platinum nanoparticles were also synthesized by reducing  $\text{H}_2\text{PtCl}_6$  with hydrazine in the w/o microemulsion consisting of  $\text{C}_{12}\text{E}_4$  (Brij 30) alone, n-heptane and water (Rivadulla et al., 1997). Absorption spectrum of the aqueous solution of  $\text{H}_2\text{PtCl}_6$  shows two different bands (at 220 nm and 260 nm). After mixing of two different microdroplets, absorption spectrum showed only one peak centered at 236 nm which is attributed to the formation of Pt nanoparticles. The position of the observed band differs from the expected one appeared at ~215 nm (Creighton & Eadon, 1991). This difference was discussed in terms of the formation of anisotropic nanoparticles (nanorods (NRs)) and the interaction between the particles (formation of aggregates). The conformation and packing of the PEG can strongly influence the accessibility of the polymer chains for interaction (the complex formation, hybridization,...) and the particle mobility (Scheme 8). The mobility of the PEG-coated gold nanoparticles is always retarded by the increased ligand density which is directly related to the particle retention and distribution between organs.



Scheme 8. Different possible configurations of PEG molecules attached to the surface of gold nanoparticles.

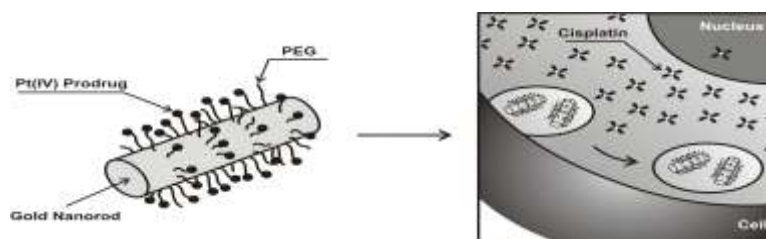
The photoinitiation mechanism of particle nucleation is complex because some or all components of the reaction system can absorb light. These molecules such as nonionic surfactant (its terminal hydroxyl groups), reducing agents or additives (dyes) are then transferred to the excited entities and participate in the charge transfer reactions and reduction processes. This complex approach was discussed by Rivadulla et al. (Rivadulla et al., 1997) who prepared platinum nanoparticles at different temperatures with/without exposure to light irradiation. They used AOT instead of PEG-based stabilizer because AOT has no terminal hydroxyl groups and only small changes appeared. However, at temperature 50 °C the reaction produces a brown color that is observed also by platinum particles obtained by hydrazine reduction, confirming the formation of colloidal Pt particles without addition of the reducing agent. Sulfonate groups of the excited ionic surfactant AOT are supposed to donate electrons, causing reduction of silver salt during irradiation and nucleate nanoparticles. Excited reactants might also take part in reduction mechanism via donation of electrons or radicals. Indeed, UV irradiation of surfactant micelles saturated with monomer initiated the microemulsion polymerization of vinyl monomers (Capek, 2014). Thus, the radicals formed within the microdroplets or the continuous phase at higher temperature or by irradiation might start the reduction of metal precursors. Furthermore, impurities in reactants may also donate electrons (the radicals) by excitation caused by the absorption of light or transformed to radical intermediates at higher temperatures (Sheu & Chen, 1988).

The inverse microemulsion (water/Triton X-100/propanol-2/cyclohexane) saturated with Pt and Ru salts provided the hybrid nanoparticles of Pt/Ru (Zhang & Chan, 2003). The particle sizes were varied in the range 2.5 - 4.6 nm by varying the precursor salt and hydrazine concentrations. At low Pt-Ru salt concentration, below 20 mM, the particles with the diameter around 2.5 nm appeared. When the Pt-Ru concentration increased above 20 mM (up to 60 mM), the size of Pt-Ru alloy nanoparticles increased to 4.0 – 4.5 nm. Beyond 60 mM the average nanoparticle size remained constant at 4.5 nm. Similar results were obtained for microdroplets stabilized with cationic surfactants (Chen & Wu, 2000). The common feature of the present studies is that the size of initial microdroplets is much larger than the size of metal nanoparticles. The particle size of the latter varied from 26 nm to 83 nm with increasing concentrations of Ru and Pt salts from 2 to 100 mM. This behavior was discussed in the following two terms: 1) For the {(Ru} + {Pt}} salts mixture below 20 mM the generation of one metal particle requires several Pt-Ru microdroplets. 2) Beyond 20 mM, a single precursor droplet saturated with Pt-Ru requires the nucleation to start the entrance of hydrazine droplets. The particle nucleation and growth are controlled by the collision among Pt-Ru-and hydrazine containing droplets. Furthermore the collision among the formed is very low because they are outnumbered by the hydrazine droplets by a factor of  $>10^4$ .

Pure palladium nanoparticles have been prepared by the reverse microemulsion consisting of {bis(N-octylethylenediamine)palladium(II) chloride ((Pd(oct-en)<sub>2</sub>)Cl<sub>2</sub>), water, chloroform and NaBH<sub>4</sub> as a reducing agent (Iida et al., 2002; Hamada et al., 2000). Monodisperse metal nanoparticles appeared at a low precursor (Pd(oct-en)<sub>2</sub>)Cl<sub>2</sub> concentration with the (water)/((Pd(oct-en)<sub>2</sub>)Cl<sub>2</sub>) ratio ( $\omega$ ) = 7.6. At a very low amount of water  $\omega < 10$ , the structure of the aggregates confirms a reverse micelle type. At a somewhat higher level of water  $\omega \geq 20$ , the classical microdroplets appeared. At  $\omega = 50$  an onset of the bicontinuous structure creates. The further variation in droplet size and shape one can obtain by using different solvents and reaction conditions. For example, the addition of methanol changed spherical to anisotropic nanoparticles. This is attributed to the variation of structures of the stabilizer/palladium complexes and microdroplets and the participation these complexes on the reaction and stabilization processes. The alkylethylenediamine/palladium complex, for example, acts as a metal precursor and a metal-particle stabilizer as well.

The spherical nanoparticles of Pt were nucleated and grew in the microdroplets stabilized by nonionic surfactant polyvinylpyrrolidone (PVP) and saturated with potassium hexachloroplatinate salt in the presence of hydrogen as a reductant (Yu & Xu, 2003). The similar procedure was used to prepare cubic platinum nanoparticles capped with oxalate (Fu et al., 2002) and tetrahedral platinum nanoparticles capped with PVP (Yu & Xu, 2003; Narayanan & El-Sayed, 2005; Narayanan & El-Sayed, 2004a; Narayanan & El-Sayed, 2004b). Polyacrylate-based stabilizer was used in the modified version of the hydrogen reduction method to produce polymer capped cubic platinum nanoparticles (Ahmadi et al., 1996; Narayanan & El-Sayed, 2004a; Narayanan & El-Sayed, 2004b; Narayanan & El-Sayed, 2004c). Capping agents based on PEG and PVP were also used to prepare and stabilize the platinum nanowires and tetrapods (Iida et al., 2002).

Min et al. have used PEGylated gold nanorods (PEG-covered AuNR, AuNR@PEG) as a carrier for platinum drug complexes (Scheme 9) (Min et al., 2010). The prodrug Pt(IV) complex was conjugated to the surface of PEG-AuNRs. On entering cells, the high reactivity of Pt(IV) prodrug via entering the cells was modified (reduced by cellular reductants, e.g. glutathione) to the divalent platinum form. Simultaneously the cisplatin can be released from the carrier matrix and/or interacts with cell biopolymers (proteins, enzymes,...). PEG-based particle stabilizer and linkage are widespread in the clinical use. For example, PEG-AuNR conjugates are highly stable, relatively noncytotoxic in vivo, and the PEGylated drugs, nanoparticles and various therapeutics can be „masked“ from the human's immune system (Veronese & Pasut, 2005). Thus as shown earlier, AuNR@PEG – platinum drug ligand conjugates enhance both the cell uptake of platinum drugs and the cytotoxicity of the conjugated cisplatin compared with cisplatin alone.

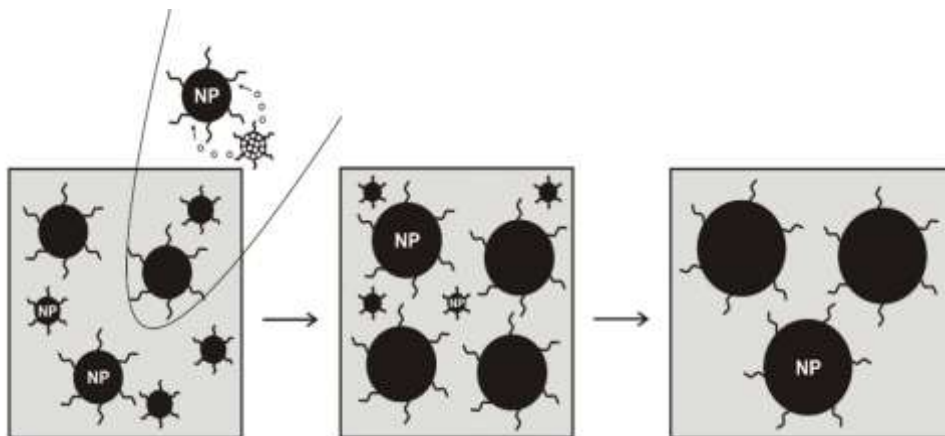


Scheme 9. Schematic illustration of AuNR@PEG-platinum ligand conjugates for drug delivery (Min et al., 2010)

#### 4. Ripening Processes

The continuous degradation of monomer dispersion mostly increases the particle size distribution. The large droplets growth on the expense of the small ones and this process is called Ostwald ripening (De Smet et al., 1997). In this

process the high surface energy of the small droplets promotes their dissolution and the dissolved material is then re-deposited on the large particles. The “Ostwald ripening” proceeds also in the colloids with metal nanoparticles or nanocrystals. This process involves the growth of large particles (crystals) on the expense of the small ones by the adsorption of atoms from the atom-saturated continuous phase. The surface metal atoms from small nanoparticles have a higher solubility than those from large nanoparticles. A group of free standing crystallites with unequal sizes in nonequilibrium form will further differentiate and redistribute themselves through the above solid–solution–solid process to achieve a more uniform size distribution (Scheme 10).



Scheme 10. Ostwald ripening process.

The particle size distribution of metal nanoparticles can be narrower by the heating of nanoparticles solution under reflux known as the “digestive ripening” (Lin et al., 1999b). This simple procedure dramatically improves the particle size distribution. Herein this approach was first successfully applied for the formation of uniform gold nanoparticles (Lin et al., 2000). The alkylthiols-decoration of nanoparticles improve the particle size distribution of gold nanoparticles, that is, for example a very polydisperse colloid by ligating the nanoparticles with dodecanethiol followed by a digestive ripening process gives a monodisperse colloid. Continuous deaggregation of the surface oligomers occurs via the incorporation of additional stabilizer molecules that helps to release the surface embryos from the particle surface. Furthermore, these oligomers may also disassemble and collide with further large particles, finally forming an irreversible particle. The energy barrier for this oligomer deaggregation from large nanoparticles (spontaneous and random deaggregation occurring throughout the solution) is high and hence requires higher degree of metastability (e.g., supersaturation) compared to that for the small nanoparticles. In the case of large nanoparticles, growth occurs on surfaces of pre-existing large nanoparticles, hence, some energy is released by the partial elimination of those pre-existing interface by their interaction with primary oligomers. This energy gain decreases the overall free energy barrier and favors the growth of large nanoparticles. Therefore, the particle growth via small-large nanoparticles interaction proceeds at the lower (super) saturation level of large nanoparticles compared to that of small nanoparticles.

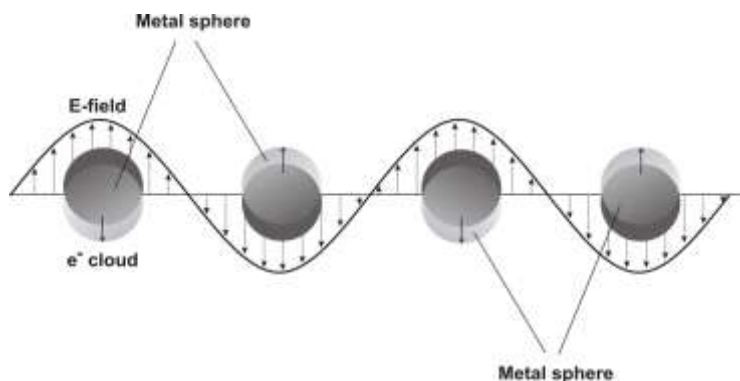
A digestive ripening process provided narrower particle distribution in the following study. The gold colloid with sizes ranging from 1 to 40 nm by heating tuned the particle size to the range of 4-4.5 nm (TEM) (Stoeva et al., 2002). The appearance of a narrow plasmon absorption peak (UV/vis absorption) with the maximum at 513 nm confirmed the presence of uniform gold nanoparticles. Without the digestive ripening a broad plasmon absorption band with no definite maximum appeared (Ferrell et al., 1985). A similar trend in the narrowing of the particle size distribution by heating of gold/toluene dispersion was reported in the next study (Lin et al., 1986). Herein the fraction of small spherical nanoparticles with sizes of about 4 nm strongly increased as well as their tendency to self-assemble into both 2D layers and 3D structures. Even the mechanism of this process is not entirely clear the surfactant-coated nanoparticles are the necessary starting material. The gold powder itself or its mixtures with various surfactant does not undergo to digestive ripening. The surfactant-capped nanoparticles take part in the diffusion of “free atoms” in solid-solvent-solid steps and this transform is much more active with the smaller nanoparticles. The surface atoms of small nanoparticles are speculated to be “much more free” to desorb into the solution than those of the large nanoparticles. The surface metal atoms of very small nanoparticles are “nearly free” to be desorbed into the continuous phase and adsorbed by solid phase of large nanoparticles (Klabunde & Mulukutla, 2001). The surfaces of both small and large nanoparticles (water- or oil-soluble metal nanoparticles) are passivated or wetted with the solute and surfactant molecules and the solubility of these surface particle entities is higher at small particles. This behavior is besides of above mentioned discussion also probably due to the fact that these nanoparticles were prepared by a “wet chemistry” procedure and therefore the solution is saturated with surfactant and free atoms. We speculate that the encapsulation of surfactant

molecules into the particle matrix might favor the discussed dissolution events. The predominant adsorption of atoms by large nanoparticles shift the equilibrium in favor of the growth of large nanoparticles. The continuous solubilization of surface particle entities leads to the saturation of solution with surfactant and free atoms. Furthermore, the free surfactant micelles can serve as vesicles for the transfer of atoms from small nanoparticles via solution to the large particles (a la multiemulsion).

The heating of gold colloids can change not only their size but also their shape. This is reason why new formed colloid may appear in different colors. For example, the red gold colloid changed to a brown color one (Lin et al., 1986; Bain et al., 1989). The color change is also a function of solvent type (acetone, toluene or their mixtures). In great excess of acetone the gold nanoparticles are strongly solvated by acetone and the bond of thiol (RSH) molecules on the particles' surface becomes weaker. Acetone (or similar solvents), with its nonbonding electron pairs, can serve as a reasonably good ligand for gold but can only compete with RSH at high acetone concentrations. Under such a condition the particle agglomeration is more favored as well as the color change. As larger volume of acetone is removed, the thiol competes better and better. This varies with the solubility of alkylthiols in solvent and it is enhanced with the long-chained thiol because it is less soluble in acetone than in toluene. Acetone acts as a weak stabilizing agent, which is substituted by alkylthiol molecules when acetone is evaporated. This ensures good dispersity of the long-chained thiol (apolar)-ligated gold particles in the toluene medium. On the contrary, the short-chained thiol (less polar)-ligated gold particles are well dispersed in the acetone medium. These studies can be also devoted to the wetting of surfactant-decorated gold nanoparticles. Toluene achieves much better wetting of the thiol molecules on the gold particles' surface compared to the more polar solvent acetone. A similar trend is expected also for the colloids in other solvents.

## 5. Optical Properties

The field of noble metal nanoparticles research has received tremendous attention due to their unique collective properties. The properties of these nanoparticles arise from their size confinement effect (Kubo, 1962). A distinct feature of small gold nanoparticles is the red color of their colloids that is caused by the surface plasmon resonance (SPR) absorption (Link & El-Sayed, 1999a). For a spherical nanoparticle much smaller than the wavelength of light, an electromagnetic field at a certain frequency induces a resonant, coherent oscillation of metal free electrons across the nanoparticle. This oscillation is known as the surface plasmon resonance (SPR) (Scheme 11). For the gold and silver nanoparticles the SPR maximum lies at visible frequencies (Link & El-Sayed, 2003; Mulvaney, 1996). The surface Plasmon oscillation of the metal electrons results in a strong enhancement of absorption and scattering of electromagnetic radiation in resonance with the SPR frequency of the studied nanoparticles, giving them intensive colors.



Scheme 11. Schematic view of the surface plasmon resonance absorption by noble metal nanoparticles (Jain et al., 2007).

Colloidal gold nanoparticles sample is ruby red in color. Mie explained this phenomenon theoretically by solving Maxwell's equation for the absorption and scattering of electromagnetic radiation by spherical particles (Mie, 1908). Gold nanoparticles with diameters  $\sim 10\text{-}20$  nm exhibit a red color and absorption peak around 520 nm (Bohren & Huffman, 1983). The frequency and cross/section of SPR absorption and scattering depend on several parameters such as the size and shape of nanoparticles, atom type, surface particle composition, particle concentration, dielectric properties of the surrounding media, and inter-particle interactions (Jain et al., 2006a). The extreme sensitivity of the bandwidth, the peak height and shape, and the position of the absorption (or scattering) maximum of SPR spectra to environmental changes has initiated the development of gold nanoparticle-based sensors (Thanh & Rosenzweig, 2002; Reynolds et al., 2000). Small gold nanoparticles with a diameter  $\leq 20$  nm show essentially absorption (Jain et al., 2006b). The relative contribution of light scattering to the total extinction of the particle increases with increasing the particle diameter above 20 nm. This behavior of the gold nanoparticles is applied for molecular labeling. The Plasmon

band shifts to longer wavelengths with increasing particle size, the change in the particle shape, the interparticle interactions and particle associations (Brause et al., 2002; Kerker, 1985; Sosa et al., 2003).

Gold nanoparticles have much higher absorption coefficients than conventional dyes. Furthermore, absorption spectra of gold nanoparticles do not undergo bleaching, that is, absorption coefficients of gold nanoparticles do not decrease with UV irradiation period. This is not the case for organic dyes that undergo bleaching and degradation. The gold nanoparticles has been already applied in colorimetric detection of analytes due to the following features: 1) the induced aggregation of gold nanoparticles attributed to the interaction with some probes changes the color of colloids and 2) , the refractive index of the AuNPs environment changes due to adsorption of biological analytes. The great enhancement of electromagnetic field at the surface of AuNPs by interaction of electrons with electromagnetic radiation offers other interesting physical properties with great potential for biodiagnostic assays (Baptista et al., 2008).

This behavior is presented in the spherical (zero-dimensional, 0D) gold nanoparticles coated with glutathione (GSH), lipoic acid (LA), DNA, bovine serum albumin (BSA) and chitosan (Figure 1). The decorated nanoparticles are monodisperse which is confirmed by a single peak in the absorbance spectra (Figure 1). The maximum of absorbance  $\lambda_{\max}$  of gold nanoparticles in the absence of a capping agent was observed to be at around 530 nm with the mean hydrodynamic diameter in the range of 20-30 nm. In the presence of all additives the absorption peaks are shifted to higher wavelength. The strongest shift in the  $\lambda_{\max}$  is observed for LA conjugate. Thus the  $\lambda_{\max}$  appeared around 540-580 nm for GSH- and 560-620 nm for LA- decorated gold nanoparticles. The nanoparticles with different sizes led to the colloid with different colors, that is, the wine red color for the bare nanoparticles changed to blue for GSH- and dark blue for LA- decorated gold nanoparticles (Ahirwal & Mitra, 2009; Bakshi et al., 2010). The color of both GSH- and LA-stabilized nanoparticles did not change with time compared to the color of bare nanoparticles.

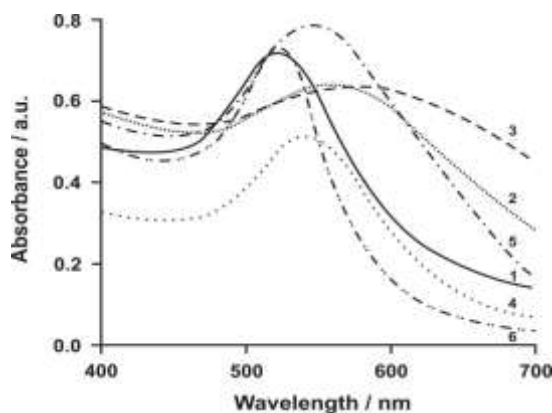


Figure 1. UV-Visible spectrum of (1) gold nanoparticles (AuNP), (2) GSH-AuNP, (3) LA-AuNP, (4) DNA-AuNP, (5) BSA-AuNP and (6) chitosan (Ahirwal & Mitra, 2009; Bakshi et al., 2010).

The further interesting feature of gold nanoparticles is their ability to efficiently quench emission from excited organic dyes located within a few nanometers of the particle surface (Lakowicz, 2001). When fluorophore probes are attached to gold surfaces, the gold surface can provide fluorescence quenching, and no organic quencher dye is required. The presence of gold or silver provides alternative nonradiative energy decay paths that can change the fluorescence quantum yield of a fluorophore. At close distances (< 5 nm) fluorescence is quenched and at longer distances (7.5–10.0 nm), it is enhanced (Lakowicz, 2001). Perez-Luna et al. (Perez-Luna et al., 2002) have used a gold surface to quench fluorescence of bound molecules and detected emission after displacement in a competitive immunoassay. Fluorescently labeled thio-oligonucleotides were attached to gold surfaces to demonstrate proof of principle for nucleic acid assays. Fluorescence from the unstructured probes can be quenched with single-stranded oligonucleotides due to their high flexibility and forming looped structures with the gold surface (Nie & Emory, 1997). Upon hybridization the double-stranded DNA is rigid and can't form looped structures to the particle surface. The major shortcoming of both solution-based and particle -based molecular beacons are the limited multiplexability (Varma-Basil et al., 2004).

Numerous assays were developed for a wide range of analytes (e.g., DNA, protein, metal ions, enzyme, and small molecular drugs) to follow photochemical and photophysical events within the studied systems. For example, Du et al. (Du et al., 2003) demonstrated quenching of hairpin DNA sequences attached to a planar gold surface, to mimic a microarray experiment, and successfully distinguished two DNA sequences, and they also started to investigate the thermodynamic and kinetic response of the sensor (Du et al., 2005). Dubretret et al. (Dubretret et al., 2001) used a hairpin loop beacon probe structure on small gold nanoparticles, while Maxwell et al. (Maxwell et al., 2002) showed that even unstructured oligonucleotide probes could be employed.

Spherical gold nanoparticles have been already discussed as the distinct colorimetric probes. The one-dimensional (nonspherical) nanoparticles have been also used to construct plasmon coupling-based colorimetric assays with novel optical characteristics (Huang et al., 2007; Link & El-Sayed, 2005). Gold nanorods possess two bands: a weaker band around 530 nm that corresponds to the transverse Plasmon oscillation and a stronger band at longer wavelengths arising from the Plasmon oscillation of electrons along the longitudinal axis of the nanorods (Link et al., 1999b). The latter band can be even shifted into the near-IR region by an increase in the nanorod aspect ratio (Huang et al., 2006). Particle association and/or agglomeration (or interparticle interaction) is accompanied with the redshift of the transverse peak and the blueshift of the longitudinal peak.

Mock and coworkers (Mock et al., 2002) studied the absorption spectra of silver nanoparticles with different sizes and shapes in the whole range of visible region. The prepared spherical and nonspherical with anisotropic silver nanoparticles with different sizes (40–120 nm) and shapes (spheres, decahedrons, triangular truncated pyramids and platelets) absorbed light in the blue, green and red part of the spectrum, respectively. The SPR peak intensity increased with size and the shift to longer wavelengths is observed at one-dimensional nanoparticles.

## 6. Conclusions

Novel hybrid pseudospherical and anisotropic nanoparticles, bimetallic triangular nanoparticles, and core@shell nanoparticles were prepared by the different procedures for various applications. Hybrid nanoparticles of gold and silver are considered to be low in toxicity, and exhibit facile surface functionalization chemistry. Furthermore, their absorption peaks are located in visible and near-infrared region. These nanoparticles provide significant plasmon tunability, chemical and surface modification properties, and significant advances in the growth into anisotropic nanostructures. Ostwald and digestive ripening provided narrower particle size distribution. The unique collective properties of noble metal nanoparticles have generated considerable interest for their use in a wide range of diverse applications. Their properties results from their large surface-to-volume ratio that strongly differ from the bulk materials. Silver and gold nanoparticles have much higher absorption coefficients than conventional dyes and their absorption spectra do not undergo bleaching. The gold nanoparticles has been already applied in colorimetric detection of analytes due to the following features: 1) the induced aggregation of gold nanoparticles attributed to the interaction with some probes changes the color of colloids and 2) , the refractive index of the AuNPs environment changes due to adsorption of biological analytes. The heating of silver gold colloids can change not only their size but also their shape. This is reason why new formed colloid may appear in different colors. The color change is also a function of solvent type. The passivation of metal particles with polar and apolar organic solvents might lead to the gold-solvent colloid which has particles well dispersed in polar or apolar solvents.

## Acknowledgements

This research is supported by the VEGA grants 2/0040/14 and 2/0152/13 and APVV-0125-11 grant.

## Nomenclature

0D	zero-dimensional
1D	one-dimensional
AFM	atomic force microscopy
AgNPs	silver nanoparticles
AOT	sodium bis(2-ethylhexyl)sulfosuccinate
AuNPs	gold nanoparticles
CA	citric acid
C <sub>12</sub> E <sub>4</sub> (Brij 30), C <sub>12</sub> E <sub>5</sub> , C <sub>12</sub> E <sub>6</sub> , C <sub>12</sub> E <sub>4</sub> (Brij 30)	poly(ethylene glycol)monododecyl ethers
CTAB	cetyltrimethyl ammonium bromide
DB24C8	dibenzo(24)crown-8
DBA	dibenzylammonium
DDAB	didodecyltrimethylammonium bromide
Dx	dextran
H <sub>2</sub> PtCl <sub>6</sub>	hexachloroplatinum acid
HRTEM	high resolution TEM
LNTs	lipid nanotubes

MSNPs	mesoporous silica nanoparticles
NMOFs	nanoscale metal–organic frameworks
NRs	nanorods
OPS	oligopolystyrene
OR	Oswald ripening
PEG	poly(ethylene glycol)
PMAA	poly(methacrylic acid)
PtCl <sub>6</sub> <sup>2-</sup>	platinum salt
PVP	polyvinylpyrrolidone
SPIO	superparamagnetic iron oxide
SPIO-DB24C8	crownether-decorated superparamagnetic iron oxide nanoparticles
TEM	transmission electron microscopy
TEOS	tetraethyl orthosilicate
ω	ratio of (water)/(surfactant

## References

- Ahirwal, G. K., & Mitra, C. K. (2009). Direct electrochemistry of horseradish peroxidase-gold nanoparticles conjugate. *Sensors*, *9*(2), 881-894. <http://dx.doi.org/10.3390/s90200881>
- Ahmadi, T. S., Wang, Z. L., Green, T. C., Henglein, A., & El-Sayed, M. A. (1996). Shape-Controlled Synthesis of Colloidal Platinum Nanoparticles. *Science*, *272*, 1924-1926. <http://dx.doi.org/10.1126/science.272.5270.1924>
- Badjic, J. D., Ronconi, C. M., Stoddart, J. F., Balzani, V., Silvi, S., & Credi, A. (2006). Operating molecular elevators. *Journal of the American Chemical Society*, *128*, 1489-1499. <http://dx.doi.org/10.1021/ja0543954>
- Bain, C. D., Evall, J., & Whitesides, G. M. (1989). Formation of Monolayers by the Coadsorption of Thiols on Gold: Variation in the Head Group, Tail Group, and Solven. *Journal of the American Chemical Society*, *111*, 7155-7164. <http://dx.doi.org/10.1021/ja00200a039>
- Bakshi, M. S., Jaswal, V. S., Possmayer, F., & Petersen, N. O. (2010). Solution Phase Interactions Controlled Ordered Arrangement of Gold Nanoparticles in Dried State. *Journal of Nanoscience and Nanotechnology*, *10*, 1747-1756. <http://dx.doi.org/10.1166/jnn.2010.2050>
- Baptista, P., Pereira, E., Eaton, P., Doria, G., Miranda, A., Gomes, I., Quaresma, P., & Franco, R. (2008). Gold nanoparticles for the development of clinical diagnosis methods. *Analytical and Bioanalytical Chemistry*, *391*, 943-950. <http://dx.doi.org/10.1007/s00216-007-1768-z>
- Boal, A. K., Ilhan, F., DeRouchev, J. E., Thurn-Albrecht, T., Russell, T. P., & Rotello, V. M. (2000). Self-assembly of nanoparticles into structured spherical and network aggregates. *Nature*, *404*, 746-748. <http://dx.doi.org/10.1038/35008037>
- Bohren, C. F., & Huffman, D. R. (1983). *Absorption and Scattering of Light by Small Particles*; John Wiley & Sons: New York, 544.
- Brause, R., Moeltgen, H., & Kleinermanns, K. (2002). Characterization of laser-ablated and chemically reduced silver colloids in aqueous solution by UV/VIS spectroscopy and STM/SEM microscopy. *Applied Physics B: Lasers and Optics*, *75*, 711-716. <http://dx.doi.org/10.1007/s00340-002-1024-3>
- Brousseau, L. C., Novak, J. P., Marinakos, S. M., & Feldheim, D. L. (1999). Assembly of phenylacetylene-bridged gold nanocluster dimers and trimers. *Advanced Materials*, *11*, 447-449. [http://dx.doi.org/10.1002/\(SICI\)1521-4095\(199904\)11:6<447::AID-ADMA447>3.0.CO;2-I](http://dx.doi.org/10.1002/(SICI)1521-4095(199904)11:6<447::AID-ADMA447>3.0.CO;2-I)
- Brust, M., Walker, M., Bethell, D., Schiffrin, D. J., & Whyman, R. (1994). Synthesis of thiol-derivatised gold nanoparticles in a two-phase Liquid–Liquid system. *Journal of the Chemical Society, Chemical Communications*, 801-802. <http://dx.doi.org/10.1039/c39940000801>
- Capek, I. (2004). Preparation of metal nanoparticles in water-in-oil (w/o) microemulsions. *Advances in Colloid and Interface Science*, *110*, 49-74. <http://dx.doi.org/10.1016/j.cis.2004.02.003>
- Capek, I. (2014). On photoinduced polymerization of acrylamide. *Designed Monomers and Polymers*, *17*, 356-363.

<http://dx.doi.org/10.1080/15685551.2013.840510>

- Chak, C. P., Xuan, S., Mendes, P. M., Yu, J. C., Cheng, C. H. K., & Leung, K. C. F. (2009). Discrete functional gold nanoparticles: hydrogen bond-assisted synthesis, magnetic purification, supramolecular dimer and trimer formation. *ACS Nano*, *3*, 2129-2138. <http://dx.doi.org/10.1021/nn9005895>
- Chen, D. H., & Wu, S. H. (2000). Synthesis of Nickel Nanoparticles in Water-in-Oil Microemulsions. *Chemistry of Materials*, *12*, 1354-1360. <http://dx.doi.org/10.1021/cm991167y>
- Chen, J., Herricks, T., Geissler, M., & Xia, Y. (2004). Single-crystal nanowires of platinum can be synthesized by controlling the reaction rate of a polyol process. *Journal of the American Chemical Society*, *126*, 10854-10855. <http://dx.doi.org/10.1021/ja0468224>
- Creighton, A., & Eadon, D. (1991). Ultraviolet-visible absorption spectra of the colloidal metallic elements. *Journal of the Chemical Society, Faraday Transactions*, *87*, 3881-3891. <http://dx.doi.org/10.1039/ft9918703881>
- De Smet, Y., Deriemaeker, L., & Finsy, R. (1997). A Simple Computer Simulation of Ostwald Ripening. *Langmuir*, *13*, 6884-6888. <http://dx.doi.org/10.1021/la970379b>
- Du, H., Disney, M. D., Miller, B. L., & Krauss, T. D. (2003). Hybridization-based unquenching of DNA hairpins on Au surfaces: prototypical "molecular beacon" biosensors. *Journal of the American Chemical Society*, *125*, 4012-4013. <http://dx.doi.org/10.1021/ja0290781>
- Du, H., Strohsahl, C. M., Camera, J., Miller, B. L., & Krauss, T. D. (2005). Sensitivity and specificity of metal surface-immobilized "molecular beacon" biosensors. *Journal of the American Chemical Society*, *127*, 7932-7940. <http://dx.doi.org/10.1021/ja042482a>
- Dubertret, B., Calame, M., & Libchaber, A. J. (2001). Single-mismatch detection using gold-quenched fluorescent oligonucleotides. *Nature Biotechnology*, *19*, 365-370. <http://dx.doi.org/10.1038/86762>
- Feldmann, C. (2003). Polyol-Mediated Synthesis of Nanoscale Functional Materials. *Advanced Functional Materials*, *13*, 101-107. <http://dx.doi.org/10.1002/adfm.200390014>
- Ferrell, T. L., Callcott, T. A., & Warmark, R. (1985). Plasmons and surfaces. *American Scientist*, *73*, 344-353.
- Fletcher, P. D. I., Howe, A. M., & Robinson, B. H. (1987). The kinetics of solubilisate exchange between water droplets of a water-in-oil microemulsion. *Journal of the Chemical Society, Faraday Transactions*, *1*(83), 985-1006. <http://dx.doi.org/10.1039/f19878300985>
- Fu, A. H., Micheel, C. M., Cha, J., Chang, H., Yang, H., & Alivisatos, A. P. (2004). Discrete nanostructures of quantum dots/Au with DNA. *Journal of the American Chemical Society*, *126*, 10832-10833. <http://dx.doi.org/10.1021/ja046747x>
- Fu, X., Wang, Y., Wu, N., Gui, L., & Yang, Y. (2002). Shape-Selective Preparation and Properties of Oxalate-Stabilized Pt Colloid. *Langmuir*, *18*, 4619-4624. <http://dx.doi.org/10.1021/la020087x>
- Fu, Y., Zhang, J., & Lakowicz, J. R. (2009). Silver-enhanced fluorescence emission of single quantum dot nanocomposites. *Chemical Communications*, 313-315. <http://dx.doi.org/10.1039/B816736B>
- Glomm, W. R. J. (2005). Functionalized Gold Nanoparticles for Applications in Bionanotechnology. *Journal of Dispersion Science and Technology*, *26*, 389-414. <http://dx.doi.org/10.1081/DIS-200052457>
- Gole, A., Agarwal, N., Nagaria, P., Wyatt, M. D., & Murphy, C. J. (2008). One-pot synthesis of silica-coated magnetic plasmonic tracer nanoparticles. *Chemical Communications*, 6140-6142. <http://dx.doi.org/10.1039/b814915a>
- Grainger, D. W., & Castner, D. G. (2008). Nanobiomaterials and Nanoanalysis: Opportunities for Improving the Science to Benefit Biomedical Technologies. *Advanced Materials*, *20*, 867-877. <http://dx.doi.org/10.1002/adma.200701760>
- Hamada, K., Hatanaka, K., Kawai, T., & Konno, K. (2000). Synthesis of Nanosize Pt Particles by Direct Addition of Hydrazine in Ionic Reversed Micelle Systems. *Shikizai Kyokaiishi*, *73*, 385-390. <http://dx.doi.org/10.4011/shikizai1937.73.385>
- Herricks, T., Chen, J., & Xia, Y. (2004). Polyol synthesis of platinum nanoparticles: control of morphology with sodium nitrate. *Nano Letters*, *4*(12), 2367-2371. <http://dx.doi.org/10.1021/nl048570a>
- Hu, J., Wen, Z., Wang, Q., Yao, Q., Zhang, Q., Zhou, J., & Li, J. (2006). Controllable Synthesis and Enhanced Electrochemical Properties of Multifunctional Au<sub>core</sub>Co<sub>3</sub>O<sub>4</sub>shell Nanocubes. *Journal of Physical Chemistry B*, *110*, 24305-24310. <http://dx.doi.org/10.1021/jp063216h>

- Huang, X., El-Sayed, I. H., Qian, W., & El-Sayed, M. A. (2006). Cancer Cell Imaging and Photothermal Therapy in the Near-Infrared Region by Using Gold Nanorods. *Journal of the American Chemical Society*, *128*, 2115-2120. <http://dx.doi.org/10.1021/ja057254a>
- Huang, Y. F., Lin, Y. W., & Chang, H. T. (2007). Control of the surface charges of Au-Ag nanorods: selective detection of iron in the presence of poly(sodium 4-stryenesulfonate). *Langmuir*, *23*, 12777-12781. <http://dx.doi.org/10.1021/la701668e>
- Hunter, R. J. (2004). *Foundations of Colloid Science*. Oxford University Press: New York.
- Iida, M., Ohkawa, S., Er, H., Asaoka, N., & Yoshikawa, H. (2002). Formation of Palladium(0) Nanoparticles from a Microemulsion System Composed of Bis (N-octylethylenediamine)palladium(II) Chloride Complex. *Chemistry Letters*, *10*, 1050-1051. <http://dx.doi.org/10.1246/cl.2002.1050>
- Ingelsten, H. H., Bagwe, R., Palmqvist, A., Skoglundh, M., Svanberg, C., Holmberg, K., & Shah, D. O. (2001). Kinetics of the formation of nano-sized platinum particles in water-in-oil microemulsions. *Journal of Colloid and Interface Science*, *241*, 104-111. <http://dx.doi.org/10.1006/jcis.2001.7747>
- Jain, P. K., El-Sayed, I. H., & El-Sayed, M. A. (2007). Au nanoparticles target cancer. *Nano Today*, *2*, 18-29. [http://dx.doi.org/10.1016/S1748-0132\(07\)70016-6](http://dx.doi.org/10.1016/S1748-0132(07)70016-6)
- Jain, P. K., Eustis, S., & El-Sayed, M. A. (2006a). Plasmon Coupling in Nanorod Assemblies: Optical Absorption, Discrete Dipole Approximation Simulation, and Exciton-Coupling Model. *Journal of Physical Chemistry B*, *110*, 18243-18253. <http://dx.doi.org/10.1021/jp063879z>
- Jain, P. K., Huang, X., El-Sayed, I. H., & El-Sayed, M. A. (2008). Noble metals on the nanoscale: optical and photothermal properties and some applications in imaging, sensing, biology, and medicine. *Accounts of Chemical Research*, *41*, 1578-1586. <http://dx.doi.org/10.1021/ar7002804>
- Jain, P. K., Lee, K. S., El-Sayed, I. H., & El-Sayed, M. A. (2006b). Calculated absorption and scattering properties of gold nanoparticles of different size, shape, and composition: applications in biological imaging and biomedicine. *Journal of Physical Chemistry B*, *110*, 7238-7248. <http://dx.doi.org/10.1021/jp057170o>
- Jiang, J., Gu, H., Shao, H., Devlin, E., Papaefthymiou, G. C., & Ying, J. Y. (2008). Bifunctional Fe<sub>3</sub>O<sub>4</sub>-Ag heterodimer nanoparticles for two-photon fluorescence imaging and magnetic manipulation. *Advanced Materials*, *20*, 4403-4407. <http://dx.doi.org/10.1002/adma.200800498>
- Kerker, M. (1985). The optics of colloidal silver: something old and something new. *Journal of Colloid and Interface Science*, *105*, 297-314. [http://dx.doi.org/10.1016/0021-9797\(85\)90304-2](http://dx.doi.org/10.1016/0021-9797(85)90304-2)
- Klabunde, K. J., & Mulukutla, R. S., (2001). *Nanoscale Materials in Chemistry*; K. J. Klabunde, ed. Wiley Interscience: New York Chapt, 7, 223. <http://dx.doi.org/10.1002/0471220620>
- Korth, B. D., Keng, P., Shim, I. B., Tang, C., Kowalewski, T., & Pyun, J. (2008). Synthesis, Assembly and Functionalization of Polymer Coated Ferromagnetic Nanoparticles. *ACS Nano*, *996*, 272-285. <http://dx.doi.org/10.1021/bk-2008-0996.ch020>
- Kubo, R. (1962). Electronic properties of metallic fine particles I. *Journal of the Physical Society of Japan*, *17*, 975-986. <http://dx.doi.org/10.1143/JPSJ.17.975>
- Kulakovich, O., Strekal, N., Yaroshevich, A., Maskevich, S., Gaponenko, S., Nabiev, I., Woggon, U., & Artemyev, M. (2002). Enhanced Luminescence Of Cdse Quantum Dots On Gold Colloids. *Nano Letters*, *2*, 1449-1452. <http://dx.doi.org/10.1021/nl025819k>
- Lakowicz, J. R. (2001). Radiative decay engineering: biophysical and biomedical applications. *Analytical Biochemistry*, *298*, 1-24. <http://dx.doi.org/10.1006/abio.2001.5377>
- Li, X. M., de Jong, M. R., Inoue, K., Shinkai, S., Huskens, J., & Reinhoudt, D. N. (2001). Formation of gold colloids using thioether derivatives as stabilizing ligands. *Journal of Materials Chemistry*, *11*, 1919-1923. <http://dx.doi.org/10.1039/b101686p>
- Lin, S., Franklin, M. T., & Klabunde, K. J. (1986). Nonaqueous colloidal gold. Clustering of metal atoms in organic media. *Langmuir*, *2*, 259-260. <http://dx.doi.org/10.1021/la00068a027>
- Lin, X. M., Sorensen, C. M., & Klabunde, K. J. (2000). Digestive ripening, nanophase segregation and superlattice formation in gold nanocrystal colloids. *Journal of Nanoparticle Research*, *2*, 157-164. <http://dx.doi.org/10.1023/A:1010078521951>
- Lin, X. M., Sorensen, C. M., Klabunde, K. J., & Hajipanayis, G. C. (1999a). Control of Cobalt Nanoparticle Size by the

- Germ Growth Method in Inverse Micelle System: Size Dependent Magnetic Properties. *Journal of Materials Research*, 14, 1542-1547. <http://dx.doi.org/10.1557/JMR.1999.0207>
- Lin, X. M., Wang, G. M., Sorensen, C. M., & Klabunde, K. J. (1999b). Formation and dissolution of gold nanocrystal superlattices in a colloidal solution. *Journal of Physical Chemistry B*, 103(26), 5488-5492. <http://dx.doi.org/10.1021/jp990729y>
- Link, S., & El-Sayed, M. A. (1999a). Size and temperature dependence of the plasmon absorption of colloidal gold nanoparticles. *Journal of Physical Chemistry B*, 103, 4212-4217. <http://dx.doi.org/10.1021/jp984796o>
- Link, S., & El-Sayed, M. A. (2003). Optical properties and ultrafast dynamics of metallic nanocrystals. *Annual Review of Physical Chemistry*, 54, 331-366. <http://dx.doi.org/10.1146/annurev.physchem.54.011002.103759>
- Link, S., & El-Sayed, M. A. (2005). Simulation of the optical absorption spectra of gold nanorods as a function of their aspect ratio and the effect of the medium dielectric constant. *Journal of Physical Chemistry B*, 109, 10531-10532. <http://dx.doi.org/10.1021/jp058091f>
- Link, S., Mohamed, M. B., & El-Sayed, M. A. (1999b). Simulation of the optical absorption spectra of gold nanorods as a function of their aspect ratio and the effect of the medium dielectric constant. *Journal of Physical Chemistry B*, 103, 3073-3077. <http://dx.doi.org/10.1021/jp990183f>
- Maxwell, D. J., Taylor, J. R., & Nie, S. (2002). Self-assembled nanoparticle probes for recognition and detection of biomolecules. *Journal of the American Chemical Society*, 124, 9606-9612. <http://dx.doi.org/10.1021/ja025814p>
- Maye, M. M., Chun, S. C., Han, L., Rabinovich, D., & Zhong, C. J. (2002). Novel spherical assembly of gold nanoparticles mediated by a tetradentate thioether. *Journal of the American Chemical Society*, 124, 4958-4959. <http://dx.doi.org/10.1021/ja025724k>
- Mie, G. (1908). Contributions to the optics of turbid media, particularly of colloidal metal solutions. *Annals of Physics*, 25, 377-445. <http://dx.doi.org/10.1002/andp.19083300302>
- Min, Y., Mao, C., Xu, D., Wang, J., & Liu, Y. (2010). Gold nanorods for platinum based prodrug delivery. *Chemical Communications*, 46, 8424-8426. <http://dx.doi.org/10.1039/c0cc03108a>
- Mock, J. J., Barbic, M., Smith, D. R., Schultz, D. A., & Schultz, S. (2002). Shape effects in plasmon resonance of individual colloidal silver nanoparticles. *Journal of Chemical Physics*, 116, 6755-6759. <http://dx.doi.org/10.1063/1.1462610>
- Mock, J. J., Hill, R. T., Degiron, A., Zauscher, S., Chilkoti, A., & Smith, D. R. (2008). Distance-dependent plasmon resonant coupling between a gold nanoparticle and gold film. *Nano Letters*, 8, 2245-2252. <http://dx.doi.org/10.1021/nl080872f>
- Modi, A., Koratkar, N., Lass, E., Wei, B. Q., & Ajayan, P. M. (2003). Miniaturized gas ionization sensors using carbon nanotubes. *Nature*, 424, 171-174. <http://dx.doi.org/10.1038/nature01777>
- Mulvaney, P. (1996). Surface Plasmon Spectroscopy of Nanosized Metal Particles. *Langmuir*, 12, 788-800. <http://dx.doi.org/10.1021/la9502711>
- Murphy, C. J., & Jana, N. R. (2002). Controlling the Aspect Ratio of Inorganic Nanorods and Nanowires. *Advanced Materials*, 14, 80-82. [http://dx.doi.org/10.1002/1521-4095\(20020104\)14:1<80::AID-ADMA80>3.0.CO;2-#](http://dx.doi.org/10.1002/1521-4095(20020104)14:1<80::AID-ADMA80>3.0.CO;2-#)
- Nam, K. T., Kim, D. W., Yoo, P. J., Chiang, C. Y., Meethong, N., Hammond, P. T., Chiang, Y. M., & Belcher, A. M. (2006). Virus-enabled synthesis and assembly of nanowires for lithium ion battery electrodes. *Science*, 312, 885-888. <http://dx.doi.org/10.1126/science.1122716>
- Narayanan, R., & El-Sayed, M. A. (2004a). Shape-Dependent Catalytic Activity of Platinum Nanoparticles in Colloidal Solution. *Nano Letters*, 4(7), 1343-1348. <http://dx.doi.org/10.1021/nl0495256>
- Narayanan, R., & El-Sayed, M. A. (2004b). Effect of Nanocatalysis in Colloidal Solution on the Tetrahedral and Cubic Nanoparticle SHAPE: Electron-Transfer Reaction Catalyzed by Platinum Nanoparticles. *Journal of Physical Chemistry B*, 108(18), 5726-5733. <http://dx.doi.org/10.1021/jp049378o>
- Narayanan, R., & El-Sayed, M. A. (2004c). Changing Catalytic Activity during Colloidal Platinum Nanocatalysis Due to Shape Changes: Electron-Transfer Reaction. *Journal of the American Chemical Society*, 126(23), 7194-7195. <http://dx.doi.org/10.1021/ja0486061>
- Narayanan, R., & El-Sayed, M. A. (2005). Effect of colloidal nanocatalysis on the metallic nanoparticle shape: the Suzuki reaction. *Langmuir*, 21(5), 2027-2033. <http://dx.doi.org/10.1021/la047600m>
- Nie, S., & Emory, S. R. (1997). Probing Single Molecules and Single Nanoparticles by Surface-Enhanced Raman

- Scattering. *Science*, 275, 1102-1106. <http://dx.doi.org/10.1126/science.275.5303.1102>
- Park, J. H., von Maltzahn, G., Ruoslahti, E., Bhatia, S. N., & Sailor, M. (2008). Micellar hybrid nanoparticles for simultaneous magnetofluorescent imaging and drug delivery. *Angewandte Chemie International Edition*, 47, 7284-7288. <http://dx.doi.org/10.1002/anie.200801810>
- Perez-Luna, V. H., Yang, S., Rabinovich, E. M., Buranda, T., Sklar, L. A., Hampton, P. D., & López, G. P. (2002). Fluorescence biosensing strategy based on energy transfer between fluorescently labeled receptors and a metallic surface. *Biosensors and Bioelectronics*, 17, 71-78. [http://dx.doi.org/10.1016/S0956-5663\(01\)00260-3](http://dx.doi.org/10.1016/S0956-5663(01)00260-3)
- Pons, T., Medintz, I. L., Sapsford, K. E., Higashiya, S., Grimes, A. F., English, D. S., & Mattoussi, H. (2007). On the quenching of semiconductor quantum dot photoluminescence by proximal gold nanoparticles. *Nano Letters*, 10, 3157-3164. <http://dx.doi.org/10.1021/nl071729+>
- Reynolds, R. A., Mirkin, C. A., & Letsinger, R. L. (2000). A gold nanoparticle/latex microsphere-based colorimetric oligonucleotide detection method. *Pure and Applied Chemistry*, 72, 229-235. <http://dx.doi.org/10.1351/pac200072010229>
- Rieter, W. J., Kim, J. S., Taylor, K. M. L., An, H., Tarrant, T., & Lin, W. (2007). Hybrid silica nanoparticles for multimodal imaging. *Angewandte Chemie International Edition*, 46, 3680-3682. <http://dx.doi.org/10.1002/anie.200604738>
- Rivadulla, J. F., Vergara, M. C., Blanco, M. C., Lopez-Quintela, M. A., & Rivas, J. (1997). Optical Properties of Platinum Particles Synthesized in Microemulsions. *Journal of Physical Chemistry B*, 101, 8997-9004. <http://dx.doi.org/10.1021/jp970528z>
- Sathe, T. R., Agrawal, A., & Nie, S. (2006). Mesoporous silica beads embedded with semiconductor quantum dots and iron oxide nanocrystals: dual-function microcarriers for optical encoding and magnetic separation. *Analytical Chemistry*, 78, 5627-5632. <http://dx.doi.org/10.1021/ac0610309>
- Selvan, S. T., Patra, P. K., Ang, C. Y., & Ying, J. Y. (2007). Synthesis of silica-coated semiconductor and magnetic quantum dots and their use in the imaging of live cells. *Angewandte Chemie International Edition*, 46, 2448-2452. <http://dx.doi.org/10.1002/anie.200604245>
- Shelimov, B. N., Lambert, J. F., Che, M., & Didillon, B. (2000). Molecular-level studies of transition metal-support interactions during the first steps of catalysts preparation: platinum speciation in the hexachloroplatinate/alumina system. *Journal of Molecular Catalysis A: Chemical*, 158, 91-99. [http://dx.doi.org/10.1016/S1381-1169\(00\)00047-9](http://dx.doi.org/10.1016/S1381-1169(00)00047-9)
- Sheu, E. Y., & Chen, S. H. (1988). Thermodynamic analysis of polydispersity in ionic micellar systems and its effect on small-angle neutron scattering data treatment. *Journal of Physical Chemistry*, 92, 4466-4474. <http://dx.doi.org/10.1021/j100326a044>
- Shon, Y. S., Mazzitelli, C., & Murray, R. W. (2001). Unsymmetrical Disulfides and Thiol Mixtures Produce Different Mixed Monolayer-Protected Gold Clusters. *Langmuir*, 17, 7735-7741. <http://dx.doi.org/10.1021/la015546t>
- Sosa, I. O., Noguez, C., & Barrera, R. G. (2003). Optical Properties of Metal Nanoparticles with Arbitrary Shapes. *Journal of Physical Chemistry B*, 107, 6269-6275. <http://dx.doi.org/10.1021/jp0274076>
- Stöber, W., Fink, A., & Bohn, E. (1968). Controlled growth of monodisperse silica spheres in the micron size range. *Journal of Colloid and Interface Science*, 26, 62-69. [http://dx.doi.org/10.1016/0021-9797\(68\)90272-5](http://dx.doi.org/10.1016/0021-9797(68)90272-5)
- Stoeva, S., Klabunde, K. J., Sorensen, C. M., & Dragieva, I. (2002). Gram-Scale Synthesis of Monodisperse Gold Colloids by the Solvated Metal Atom Dispersion Method and Digestive Ripening and Their Organization into Two- and Three-Dimensional Structures. *Journal of the American Chemical Society*, 124, 2305-2311. <http://dx.doi.org/10.1021/ja012076g>
- Sun, S., Murray, C. B., Weller, D., Folks, L., & Moser, A. (2000). Monodisperse FePt nanoparticles and ferromagnetic FePt nanocrystal superlattices. *Science*, 287, 1989-1992. <http://dx.doi.org/10.1126/science.287.5460.1989>
- Taylor-Pashow, K. M. L., Della Rocca, J., Huxforda, R. C., & Lin, W. (2010). Hybrid nanomaterials for biomedical applications. *Chemical Communications*, 46, 5832-5849. <http://dx.doi.org/10.1039/c002073g>
- Thanh, N. T. K., & Rosenzweig, Z. (2002). Development of an Aggregation-Based Immunoassay for Anti-Protein A Using Gold Nanoparticles. *Analytical Chemistry*, 74, 1624-1628. <http://dx.doi.org/10.1021/ac011127p>
- Varma-Basil, M., El-Hajj, H., Marras, S. A., Hazbon, M. H., Mann, J. M., Connell, N. D., Kramer, F. R., & Alland, D. (2004). Molecular beacons for multiplex detection of four bacterial bioterrorism agents. *Clinical Chemistry*, 50,

1060-1062. <http://dx.doi.org/10.1373/clinchem.2003.030767>

- Veronese, F. M., & Pasut, G. (2005). PEGylation, successful approach to drug delivery. *Drug Discovery Today*, 10, 1451-1458. [http://dx.doi.org/10.1016/S1359-6446\(05\)03575-0](http://dx.doi.org/10.1016/S1359-6446(05)03575-0)
- Wang, X. D., Shen, Z. X., Sang, T., Cheng, X. B., Li, M. F., Chen, L. Y., & Wang, Z. S. (2010). Preparation of spherical silica particles by Stober process with high concentration of tetra-ethyl-orthosilicate. *Journal of Colloid and Interface Science*, 341, 23-29. <http://dx.doi.org/10.1016/j.jcis.2009.09.018>
- Wilcoxon, J. P., & Provencio, P. P. (2004). Heterogeneous Growth of Metal Clusters from Solutions of Seed Nanoparticles. *Journal of the American Chemical Society*, 126, 6402-6408. <http://dx.doi.org/10.1021/ja031622y>
- Xiang, Y., Wu, X., Liu, D., Li, Z., Chu, W., Feng, L., Zhang, K., Zhou, W., & Xie, S. (2008). Gold nanorod-seeded growth of silver nanostructures: from homogeneous coating to anisotropic coating. *Langmuir*, 24, 3465-3470. <http://dx.doi.org/10.1021/la702999c>
- Xue, C., Millstone, J. E., Li, S., & Mirkin, C. A. (2007). Plasmon-Driven Synthesis of Triangular Core-Shell Nanoprisms from Gold Seeds. *Angewandte Chemie International Edition*, 46, 8436-8439. <http://dx.doi.org/10.1002/anie.200703185>
- Yang, B., Kamiya, S., Shimizu, Y., Koshizaki, N., & Shimizu, T. (2004). Glycolipid nanotube hollow cylinders as substrates: Fabrication of one-dimensional metallic-organic nanocomposites and metal nanowires. *Chemistry of Materials*, 16, 2826-2831. <http://dx.doi.org/10.1021/cm049695j>
- Yu, H., Chen, M., Rice, P. M., Wang, S. X., White, R. L., & Sun, S. (2005). Dumbbell-like bifunctional Au-Fe<sub>3</sub>O<sub>4</sub> nanoparticles. *Nano Letters*, 5, 379-382. <http://dx.doi.org/10.1021/nl047955q>
- Yu, Y., & Xu, B. (2003). Selective formation of tetrahedral Pt nanocrystals from K<sub>2</sub>PtCl<sub>6</sub>/PVP. *Chinese Science Bulletin*, 48(23), 2589-2593. <http://dx.doi.org/10.1360/03wb0098>
- Zhai, Y., Zhai, J., Wang, Y., Guo, S., Ren, W., & Dong, S. (2009). Fabrication of iron oxide core/gold shell submicrometer spheres with nanoscale surface roughness for efficient surface-enhanced Raman scattering. *Journal of Physical Chemistry C*, 113, 7009-7014. <http://dx.doi.org/10.1021/jp810561q>
- Zhang, X., & Chan, K. Y. (2003). Water-in-Oil Microemulsion Synthesis of Platinum–Ruthenium Nanoparticles, Their Characterization and Electrocatalytic Properties. *Chemistry of Materials*, 15, 451-459. <http://dx.doi.org/10.1021/cm0203868>

## Copyrights

Copyright for this article is retained by the author(s), with first publication rights granted to the journal.

This is an open-access article distributed under the terms and conditions of the Creative Commons Attribution license (<http://creativecommons.org/licenses/by/3.0/>).